Article

Not peer-reviewed version

Correlating the Segmental-Relaxation Time of Polystyrene

C. A. Hieber *

Posted Date: 2 July 2024

doi: 10.20944/preprints202407.0223.v1

Keywords: equilibrium relaxation time; glass-rubber transition; glass-transition temperature; polystyrene; segmental-relaxation time; VFTH model

Article

Correlating the Segmental-Relaxation Time of Polystyrene

C. A. Hieber

Senior Research Associate, Retired, Sibley School of Mechanical and Aerospace Engineering, Cornell University; cah31@cornell.edu

This paper is dedicated to Avraam I. Isayev and Claude Cohen, in celebration of their 80th birthdays, and in remembrance of James F. Stevenson.

Abstract: A previous related paper dealing with the density relaxation of polystyrene (PS) has shown that the equilibrium relaxation time (τ_{eq}) has a purely exponential temperature dependence (ETD) below ≈ 100ºC. Such an ETD is now also confirmed based upon available dielectric-spectra data for PS. By combining the ETD behavior of τ_{eq} (or a_T) at low temperatures with a VFTH behavior at higher temperatures (based mainly on available recoverable-shear-compliance data), a composite correlation for τ_{eq} (or a_T) is developed which is continuous with continuous slope at a crossover temperature which is found to be 99.22ºC, where τ_{eq} = 92.15 sec. This composite representation is shown to describe (without any adjustable parameters) available independent data for the segmental-relaxation time over a finite range both above and below $T_{crossover}$ (i.e., the glass-transition temperature).

Keywords: equilibrium relaxation time; glass-rubber transition; glass-transition temperature; polystyrene; segmental-relaxation time; VFTH model

---

1. Introduction

In a recent paper by Hieber [1], based upon density relaxation of polystyrene at atmospheric pressure, it has been shown that the equilibrium relaxation time is characterized by a purely exponential temperature dependence over the experimental range available in the literature, reaching down (under equilibrium) to about 16ºC below the nominal glass-transition temperature. Such results were shown (in the same paper) to be compatible with the stress-relaxation data for polycarbonate of O'Connell and McKenna [2] as well as the equilibrium dielectric-compliance data for PVAc of Zhao and McKenna [3]; in both of these cases, the equilibrium state could again be reached down to about 16 or 17ºC below the nominal glass-transition temperature. {It is noted that "$T_{g,nominal}$" for PS is typically taken as 373ºK (i.e., essentially 100ºC), as has been done, for example, by Roland & Casalini [4] and He, et al. [5].}

In the present paper, it will be shown for polystyrene that the equilibrium relaxation time $\tau_{eq}(T)$ from Hieber [1] can be extended to temperatures above the nominal glass-transition temperature by making use of the temperature shift factor (a_T) in the glass-rubber transition obtained from available independent data (in terms of recoverable-shear-creep compliance as well as stress relaxation) from the literature. It will be shown that this composite representation for $\tau_{eq}(T)$ describes (without any adjustable parameters) available data for the segmental-correlation time of PS over a temperature range extending both above and below the (nominal) glass-transition temperature.

2. Extending $\tau_{eq}(T)$ to above T_g

Based on the results from fitting the cumulative density-relaxation data for PS from Hieber [1], the resulting equilibrium relaxation time (at atmospheric pressure) is given by

$$\tau_{eq}(T) = AA\ \exp\{-\alpha_3(T - 100°C)\} \quad (1)$$

 doi:10.20944/preprints202407.0223.v1

where

$$AA = 49.18\ \text{sec}, \alpha_3 = 0.805/°\text{C}. \quad (2)$$

Combining this with the results from Appendices A & B below, we arrive at the plot in Figure 1 in which the ordinate is a measure of the temperature sensitivity in terms of $\tau_{eq}(T)$ or a_T, namely

$$\Omega \equiv -\frac{d \ln \tau_{eq}(T)}{dT} \quad (3)$$

or

$$\Omega \equiv -\frac{d \ln a_T}{dT}. \quad (4)$$

In particular, based upon the density-relaxation data for PS from Hieber [1], we have that

$$\Omega = 0.805/°\text{C} \quad (5)$$

over the interval between 83.87°C and 100°C.

On the other hand, the three curves in Figure 1 are all based upon the VFTH model [6–8], namely,

$$a_T = BB \exp\left(\frac{CC}{(T-T_\infty)}\right) \quad (6)$$

such that

$$\Omega = \frac{CC}{(T-T_\infty)^2}. \quad (7)$$

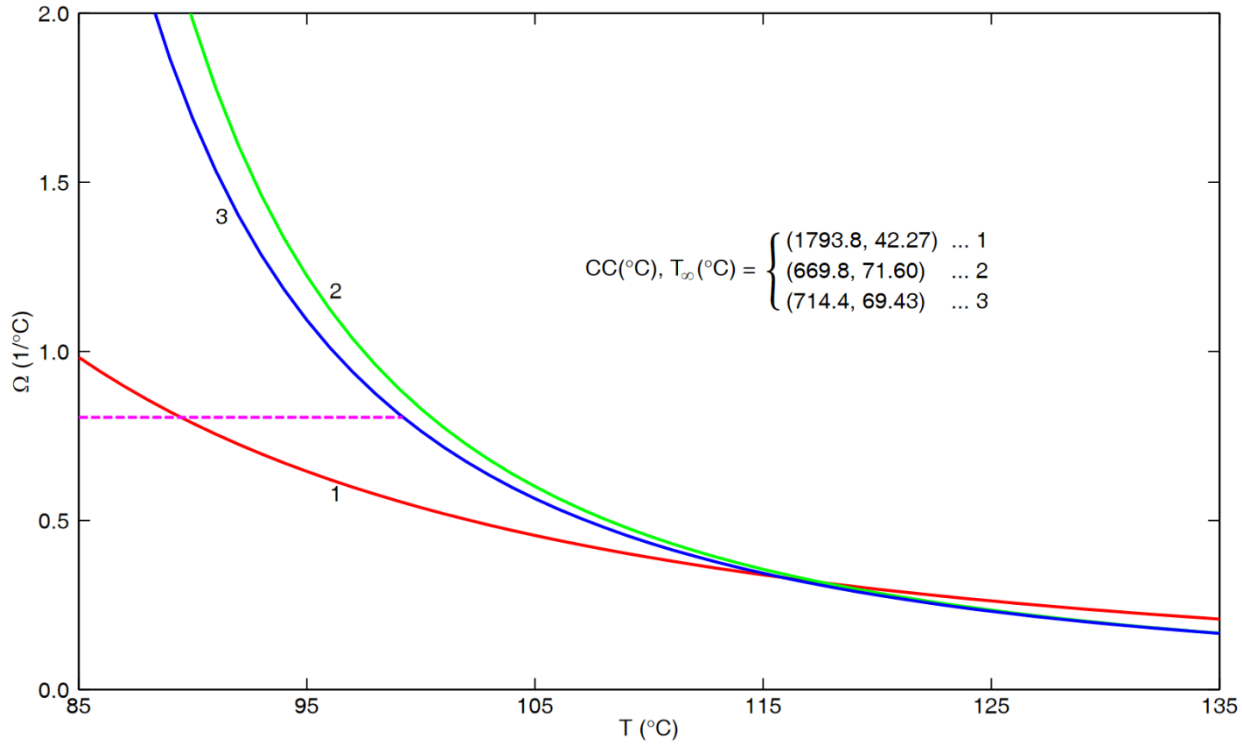

Figure 1. Results for Ω versus T. Curves based upon VFTH fits for flow regime (curve 1, from Appendix A) or glass-rubber transition (curves 2 and 3, from Appendix B). Dashed line based upon Equations (1) and (2).

In particular, curve 1 in Figure 1 is based upon cumulative data from 5 sources [9–13] for the "flow regime" reported in Appendix 1, with the measured temperatures ranging between 104.5°C and 290°C, and (CC, T∞) = (1793.8°C, 42.27°C), as given in Equation (A.2). On the other hand, curves 2 and 3 are based upon results for the "glass-rubber transition" from Appendix B involving cumulative data from 6 sources [9,14–18] in the temperature range from 100°C to 135°C, with curve 2 corresponding to (CC, T∞) = (669.8°C, 71.60°C) from Eqn. (B.1) of Appendix B and curve 3 to (CC, T∞) = (714.4°C, 69.43°C) from Equation (B.2).

Clearly, all three curves in Figure 1 have been extended to temperatures below that of the underlying data (as presented in Figures A and B). Furthermore, it is expected that the present density-relaxation results should be directly related to the "glass-rubber transition" results, both reflecting local molecular behavior, whereas the "flow-regime" results reflect long-range molecular

 doi:10.20944/preprints202407.0223.v1

motion. In addition, as documented in Appendix B, there is a basis for judging that curve 3 is more representative than curve 2. Accordingly, of especial interest in Figure 1 is the intercept of curve 3 with the dashed result given by Eqn. (5), which occurs at T = 99.22°C.

These results seem to strongly indicate that the VFTH behavior of the "glass-rubber transition" given by curve 3 in Figure 1 gets replaced by the constant value, given by Eqn. (5), at temperatures below the intersection point at 99.22°C. In turn, this indicates that the singularity (at $T \equiv T_\infty$) in the VFTH equation is only an apparent singularity.

Making use of the results in Figure 1, it seems appropriate to introduce the term "$T_{crossover}$" to denote where the dashed line and curve 3 intersect. Accordingly,

$$T_{crossover} = 99.22°C \quad (8)$$

where $\tau_{eq}(T)$ is based on Eqns. (1, 2) for $T \le T_{crossover}$ and is extended above $T_{crossover}$ by making use of curve 3 from Figure 1. That is, the resulting composite representation for $\tau_{eq}(T)$ is then given by

$$\tau_{eq}(T) = 49.18 \text{ sec} \exp\{-(0.805/°C)(T - 100°C)\} \quad (9)$$

for $T \le T_{crossover}$, such that, from Eqns. (8, 9),

$$\tau_{eq}(T_{crossover}) = 92.15 \text{ sec} \quad (10)$$

whereas, based upon curve 3 in Figure 1, for $T > T_{crossover}$ we have that

$$\tau_{eq}(T) = 92.15 \text{ sec} \exp\left\{\frac{714.4°C}{T - 69.43°C} - \frac{714.4°C}{99.22°C - 69.43°C}\right\}. \quad (11)$$

It is noted that the composite representation for $\tau_{eq}(T)$, given by Eqns. (9) & (11), is continuous with a continuous slope at $T_{crossover}$ {which follows from the definition of Ω in Eqn. (3)}. Furthermore, the value of $T_{crossover}$ in Eqn. (8) is close to the "nominal T_g" of PS, namely 100º C. Accordingly, the result in Eqn. (10) is compatible with a convention typically associated with Angell [19], namely that $T_{g,nominal}$ is where τ_{eq} is on the order of 10^2 sec.

3. Comparison with Experimental Results for the Segmental-Relaxation Time

A resulting plot for $\tau_{eq}(T)$ based upon Eqns. (9) and (11) is shown plotted in Figure 2, together with corresponding data for PS based upon various experimental techniques. Despite evident scatter, a definite correlation between the data and the composite curve (with no adjustable parameter) seems apparent.

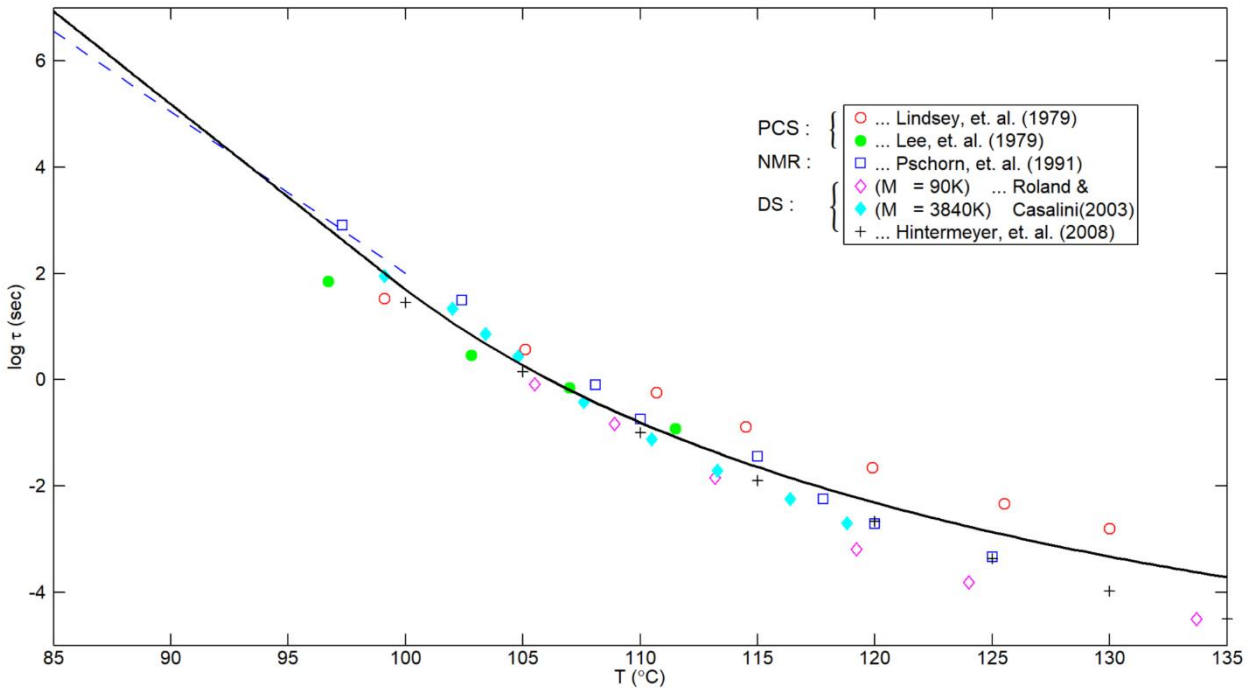

 doi:10.20944/preprints202407.0223.v1

Figure 2. Predicted curve for $\tau_{eq}(T)$ based upon Eqns. (8, 9, 11) compared with PS data based on photon-correlation spectroscopy [20,21], NMR [22], and dielectric spectroscopy [4,23]. The dashed line will be described later.

It is worth stressing that the actual level of the $\tau_{eq}(T)$ curve in Figure 2 is based upon the density-relaxation results obtained in the earlier paper, Hieber [1]. On the other hand, the extension of the curve to higher temperatures (i.e., above $T_{crossover}$) is based upon fitting cumulative results for a_T in the glass-rubber-transition region, as presented in Appendix B of the current paper.

In observing Figure 2, it is noted that the experimental results from Roland & Casalini [4] are for two PS of significantly different M_w, differing by a factor of 43, but that the corresponding results for τ_{eq} differ by no more than a half decade. For comparison, if we were dealing with viscous flow, the characteristic time would be proportional to η_0 which, for these large values of M_w, would be proportional to M_w raised to the 3.4 power. Accordingly, the respective values for the viscous-flow characteristic time for these two polymers would differ by a factor of 43 raised to the 3.4 power, i.e., 3.6×10^5. Clearly, on such a scale, the present results in Figure 2 for the two PS are essentially coincident. Stated differently, these results indicate the dramatic difference in behavior of the current results in Figure 2, relating to the local-segmental motion of PS, in contrast to the global molecular motion associated with viscous flow.

As a still further confirmation that the results in Figure 2 are independent of molecular weight (if sufficiently large), the results for PS in Figure 2(b) of Hintermeyer, et al. [23] are striking, in which the curves for "lg τ_α (sec) versus T(ºK)" are essentially coincident for the three highest molecular weights (all of NMWD), namely 96K, 243K and 546K. In fact, the corresponding data points from Hintermeyer, et al. [23] shown in the current Figure 2 have been taken from the right-most solid curve in their Figure 2(b), which is representative of the high-M_w asymptote. It is noted that Hintermeyer, et al. (23) have determined "T_g" for each of their polymers as the temperature at which τ_α equals 100 seconds. From their Table 2, the corresponding values for the above three high molecular weights were 372.6ºK (99.45ºC), 373.3ºK (100.15ºC) and 372.0ºK (98.85ºC), respectively.

4. Behavior at Higher Temperatures

Whereas Figure 2 extends to only 135ºC (reflecting the underlying related data from Appendix B), Figure 3 extends the plot to higher temperatures. In particular, the solid curve is based upon Eqns. (9) and (11), as in Figure 2, whereas the dashed curve is based upon the empirical fit obtained by He, et al. [5], namely

$$\tau_{seg,c}(T) = 0.87 \times 10^{-12} \text{ sec } \exp\left(\frac{1248^\circ C}{T - 61.55^\circ C}\right) \quad (12)$$

for the segmental-correlation time.

Preprints.org (www.preprints.org) | NOT PEER-REVIEWED | Posted: 2 July 2024 doi:10.20944/preprints202407.0223.v1

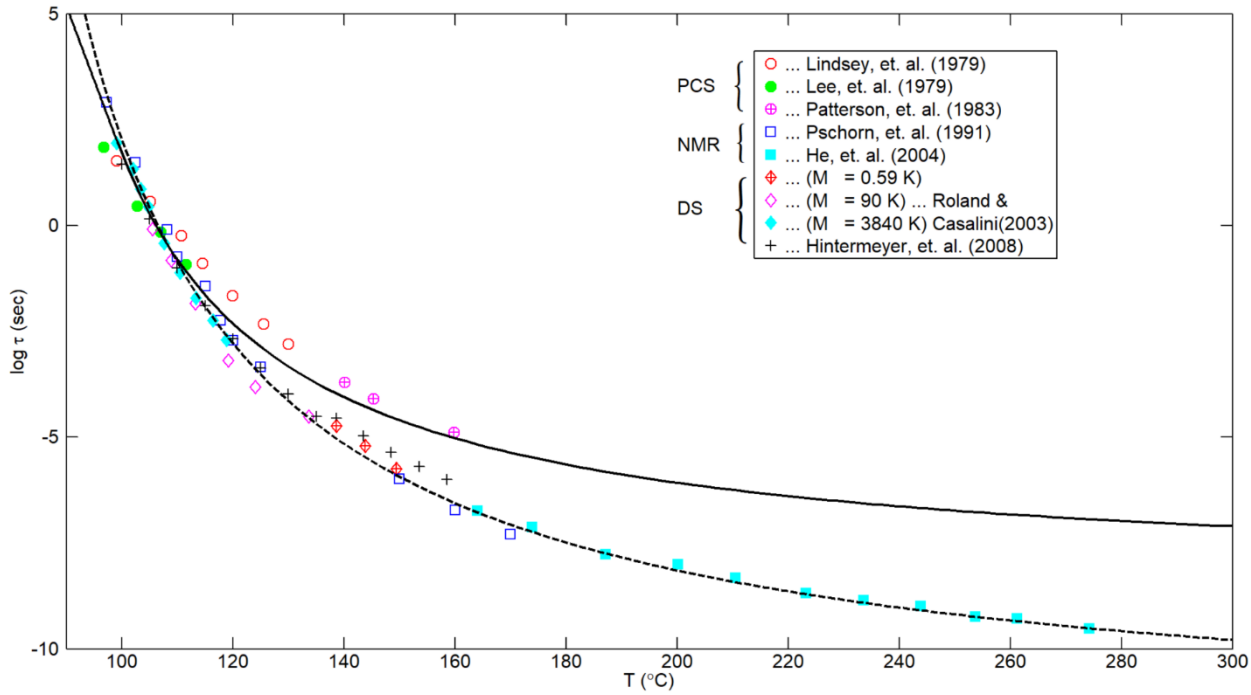

Figure 3. Predictions for the relaxation time τ(T) based on Eqns. (8, 9, 11): solid curve ; or upon Eqn. (12): dashed curve. Data based on photon-correlation spectroscopy, NMR and dielectric spectroscopy.

As noted in Figure 9 of He, et al. [5], their data, based upon three PS of low M_w (namely 2.05K, 2.31K and 11.45K), have been "horizontally shifted by ΔT_g, taking T_g = 373ºK for high molecular weight PS". In particular, the highest-temperature data point from He, et al. [5], as shown at 274ºC in the current Figure 3, corresponds to M_w = 2.05K and ΔT_g = 54ºK/ºC. Similarly, the three data points for M_w = 0.59K from Roland & Casalini [4] are taken from their Figure 4 with a ΔT_g of 119ºC. Furthermore, the five right-most data points from Hintermeyer et al. [23] shown in Figure 3 correspond to M_w = 1.350K, as presented in their Figure 11, with a ΔT_g of 59ºC.

Evidently, with the exception of the data from Patterson et al. [24], the dashed curve clearly describes the high-temperature data in Figure 3 quite well. (It should be noted that the data from Lindsey et al. [20] and Patterson et al. [24] are from the same laboratory.) As indicated in Figure 9 of He, et al. [5], their higher-temperature NMR data merge well with the lower-temperature NMR data of Pschorn et al. [22]. Furthermore (as seen in Figure 3), the correlation given by Eqn. (12) seems to be substantiated by the DS measurements obtained independently by Roland & Cassalini [4] and by Hintermeyer et al. [23].

It should be noted that Eqn. (12) gives a value of about 10^2 sec at 100ºC (often taken as the nominal glass-transition temperature for PS). This is consistent with a convention typically associated with Angell [19] which has been explicitly employed by Roland & Casalini [4] and by Hintermeyer, et al. [23].

In closing this section, one might also consider the limiting behavior of the relaxation time at a hypothetically high temperature (i.e., as $T \rightarrow \infty$), namely "τ_∞". In particular, from Eqns. (11) and (12) above we get respective values of 3.546×10^{-9} sec and 0.87×10^{-12} sec. On the other hand, Boyd & Smith [25] note that the limiting behavior (as $T \rightarrow \infty$) of various modes all seem to converge on a time scale of picoseconds (10^{-12} sec), corresponding to intramolecular and torsional oscillations. Hence, it would seem that Eqn. (12) would be more appropriate than Eqn. (11). But this is complicated by the generally accepted idea [26,27] that the WLF (or VFTH) model should get replaced by an Arrhenius behavior at sufficiently high temperatures. If that is done in the case of Eqn. (11), supposing that the VFTH in Eqn. (11) gets replaced by an Arrhenius at $T = T^*$, with their values & first derivatives being continuous, it can be verified that $\tau_\infty \cong 10^{-13}$ sec if $T^* \cong 222$°C (495ºK) and 10^{-12} sec if $T^* \cong 242$°C (515ºK). That is, these values reflect that the Arrhenius would decay more rapidly than the VFTH at

 doi:10.20944/preprints202407.0223.v1

these higher temperatures and indicate that the resulting values for τ_∞ based upon such a composite VFTH/Arrhenius model would not be unreasonable.

Further consideration of the temperature dependence in Eqn. (12), compared with the correlations for a_T in Appendices A and B, is given in Appendix C.

5. An Unanticipated Corroboration

It is noted that Ngai [28] indicates (on p. 263) that the segmental-relaxation time (τ_α) has the same temperature dependence as the creep compliance up to 384ºK (111ºC); indeed, this agrees with the present results shown in Figure 2, in which there is excellent agreement with the curve, based upon Eqns. (8, 9, 11), up to about 111ºC. On the other hand, there is also evidence that Eqn. (8, 9, 11) describes τ_α (T) even below T_g. This is based upon results from Hintermeyer, et al. [23], as follows...

In Figure 11 of Hintermeyer, et al. [23], based on dielectric-spectra data for PS, results are plotted in terms of "lg τ_α (sec)", versus "$z \equiv m\ (T/T_g - 1)$", in which "m" is the non-dimensional "fragility index". Of specific interest here is the fact that the data (all of which lie essentially above T_g) coalesce asymptotically onto a straight line as one approaches T_g (identified with where $\tau_\alpha \equiv 10^2$ sec) from above. In particular, the straight line in their Figure 11 corresponds to

$$\log \tau_\alpha = 2 - \frac{m}{T_g}\,(T\text{-}T_g) \qquad (13)$$

where τ_α is in seconds and T & T_g in ºK. From their Figure 6, m ≈ 122 for the three largest M_w and T_g ≅ 373ºK. Hence, Eqn. (13) becomes

$$\tau_\alpha\,(T) = 10^2 \text{ sec} \exp\{-(0.75/ºC)\,(T - T_g)\} \qquad (14)$$

for the PS polymers of high M_w. Indeed, the value of Ω = 0.75/ºC in Eqn. (14) agrees well (within 7%) with the value of 0.805/ºC in Equation (5). This is evidenced by the dashed line in Figure 2, which is based upon Eqn. (14) with T_g = 100ºC.

Hence, there is the strong implication that the present correlation, corresponding to Eqns. (8, 9, 11) and plotted as the curve in Figure 2 above, describes τ_α (T) for PS not only up to 111ºC but also down to perhaps 83ºC, based on the density-relaxation results for PS presented by Hieber [1], upon which the value of 0805/ºC is based.

In a similar manner, based upon the DS data of Hintermeyer, et al. [23] for polydimethylsiloxane (PDMS) and polybutadiene (PB), one obtains respective values for Ω of 1.83/ºC and 1.19/ºC, based upon the higher-M_w samples. However, since this relates to the segmental-relaxation time, the same values for Ω also pertain (essentially) to the polymers of lower M_w, as is demonstrated in Appendix D.

6. Conclusions

Main results that have been obtained in the present paper include the following:

(i) It has been shown, making use of the extensive DS data of Hintermeyer, et al. [23] for PS {as well as for Polydimethylsiloxane (PDMS) and 1, 4-Polybutadiene (PB)}, that the temperature dependence of the local segmental-relaxation time, τ_α, is purely exponential below T_g, thus confirming previous results for PS obtained by Hieber [1], based on density-relaxation considerations.

(ii) The fact that the values of 0.805/ºC in Eqn. (5) and 0.75/ºC in Eqn. (14) are in such close agreement strongly suggests that τ_{eq} (T), obtained from density-relaxation considerations, and τ_α (T), obtained from segmental-relaxation considerations, are directly related.

(iii) The results shown in Figure 2 indicate that the smooth composite correlation (with no adjustable parameters) given by Eqns. (9) and (11) describes available experimental results for the segmental-relaxation time of PS encompassing a definite temperature range both above and below the glass-transition temperature.

(iv) Based upon the results in Appendix C, there is strong evidence that, contrary to some results in the literature, the temperature dependence of τ_α(T), as given in Eqn. (12), and of a_T for the viscosity, as given in Eqns. (A.1) and (A.2), do not become coincident at higher temperatures.

Appendix A: a_T for PS in "Flow Regime"

 doi:10.20944/preprints202407.0223.v1

Shown in Figure A are results for the temperature-shift factor $a_T/a_{160°C}$ for the "flow regime" of PS based on available data. In particular, the results from Plazeck [9] are based on (long-time) shear-creep compliance whereas the remaining data are all based upon dynamic measurements in the low-frequency limit. The results from Zosel [10] are significant in that they include some eleven different PS (all with M_V>150K, of both narrow and broad molecular-weight distribution) for which a_T was essentially the same. In similar manner, Marin & Graessley [11] found that, within experimental uncertainties, their results for a_T were the same for their five PS (all of NMWD, with M_w between 37K and 670 K). Similarly, Schausberger et al. [12] found that, for five PS of NMWD (with M_w ranging between 70K and 3000K), a_T was the same within the accuracy of the measurements. In turn, the experimental results from these three investigations have been complemented in Figure A by results from Plazek [9] and Lomellini [13], extending the results to lower and higher temperatures, respectively.

Also shown in Figure A is the corresponding curve fit based upon the VFTH model [6–8]:

$$a_T/a_{TREF} = \exp\left(\frac{CC}{T\text{-}T_\infty}\right)/\exp\left(\frac{CC}{TREF\text{-}T_\infty}\right) \quad (A.1)$$

with TREF = 160°C. The best-fit values for (CC, T∞) have been determined by employing a simplex method (Nelder and Mead [29]), resulting in

CC = 1793.8°C, T∞ = 42.27°C, RMSDEV = 0.03994. (A.2)

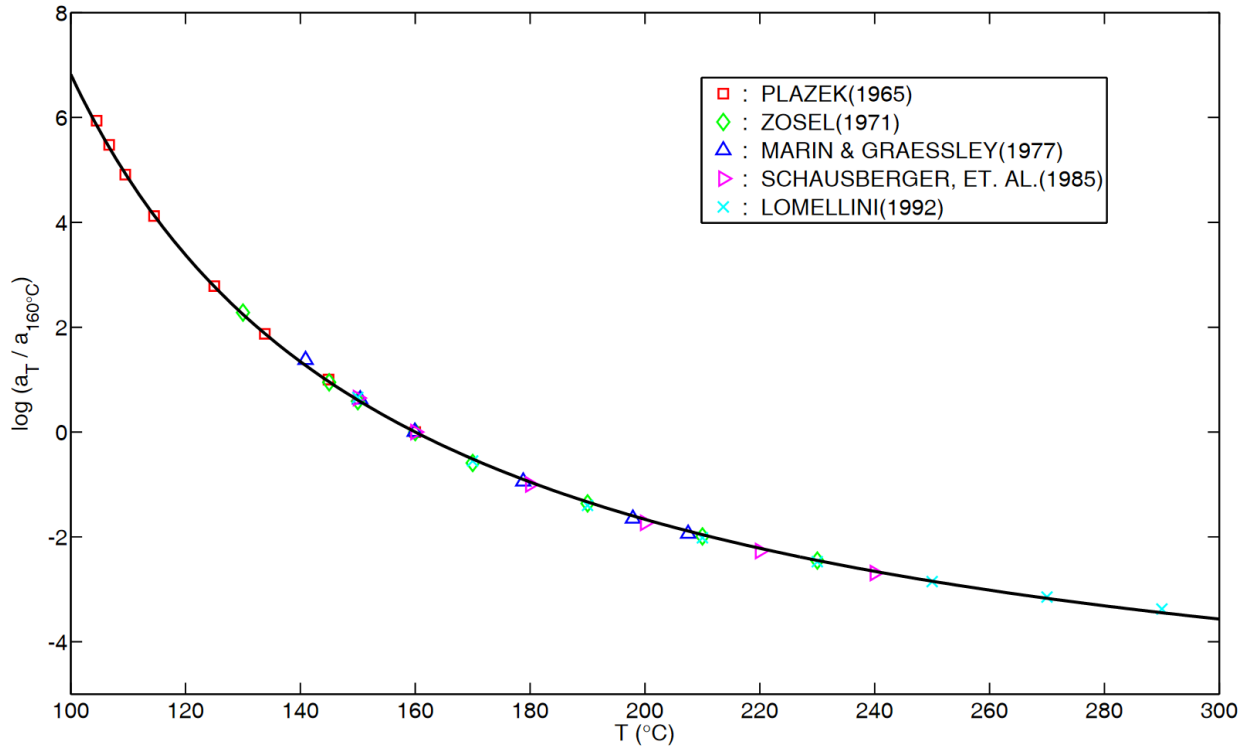

Figure A. Cumulative data for the temperature sensitivity of a_T for the flow regime of PS. Solid curve corresponds to VFTH model, Equations (A.1) and (A.2).

For comparison, it should be noted that McKenna et al. [30] have done a similar analysis of mostly different data for PS. The only viscosity measurements common to the earlier 1987 paper and the present investigation are those from Plazek [9] and Marin & Graessley [11]. Based upon fitting an extensive set of measurements, the resulting best-fit values based upon the VFTH model were found by McKenna et al. [30] to be given by

CC = 1794°C, T∞ = 42.8°C . (A.3)

 doi:10.20944/preprints202407.0223.v1

The remarkably close agreement between the model parameters in Eqns. (A.2) and (A.3) thus serves as a confirmation of the two separate investigations.

Appendix B: a_T for PS in "Glass-Rubber Transition"

Shown in Figure B are results for the temperature-shift factor, $a_T/a_{115°C}$, for the "glass-rubber-transition" regime of PS based upon available data. In particular, the results from Aklonis and Tobolsky [14] are based upon stress-relaxation measurements whereas the remaining data are all based upon recoverable-shear-creep results.

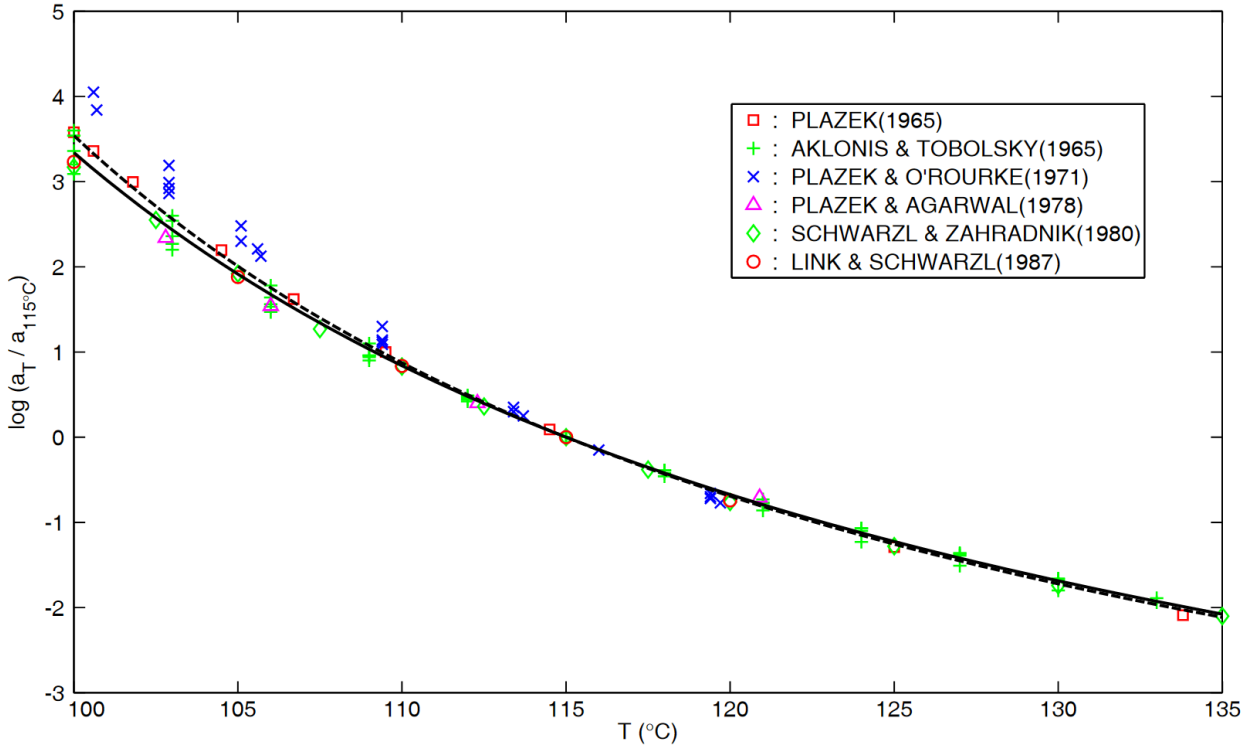

Figure B. Cumulative data for the temperature sensitivity of a_T for the glass-rubber transition of PS. Both curves are based upon VFTH model with dashed corresponding to Eqn. (B.1) and solid to Eqn. (B.2).

The two curves in Figure B are both based upon the VFTH model, as given in Eqn. (A.1), now with TREF = 115°C, with the dashed curve being the best fit of all indicated data, with

CC = 669.8°C, T_∞ = 71.60°C, RMSDEV = 0.1869 (B.1)

whereas the solid curve is the best fit when the data from Plazek and O'Rourke [15] are omitted, resulting in

CC = 714.4°C, T_∞ = 69.43°C, RMSDEV = 0.09965. (B.2)

It is noted that the RMSDEV is almost halved by omitting the data from Plazek and O'Rourke [15], indicating that the latter data are anomalous.

Although Plazek and O'Rourke [15] present tabulated results for nine PS of NMWD, only the four of highest molecular weight (94K, 189K, 600K and 800K) have been included in Figure B. (A fifth polymer, of molecular weight 47K, is actually from Plazek [9] and has been plotted in Figure B accordingly.) It is noted that the shift factor for recoverable compliance in Table II of Plazek and O'Rourke [15] is all relative to 100ºC. However, when expressed relative to 115ºC (which has been chosen as a representative value, given the temperature range of the data in Figure B), the results from Plazek and O'Rourke [15] become clearly anomalous in the lower temperature range because those data decay much more rapidly between 100 and 115ºC (as can be seen from Figure B) than the remaining experimental results from the other five sources.

 doi:10.20944/preprints202407.0223.v1

Appendix C: Further Considerations

Figure C compares results based upon the VFTH fits in Eqns. (B.2), (12) and (A.2) expressed in terms of Ω(T), a measure of temperature sensitivity, as evaluated via Equation (7). It is noted that curve 1 is based upon the fit obtained in Appendix B based (mainly) upon recoverable-shear-creep data between 100 and 135ºC. On the other hand, curves 2 and 3 should both be applicable up to 300ºC, based upon related results in Figures 3 and A, respectively. It is noted that curve 2 lies consistently above curve 1; that is, with increasing temperature, $\tau_{seg,c}$ in Eqn. (12) consistently decays faster (on a fractional basis) than a_T in Equation (B.2). On the other hand, it is noted from Figure C that curve 3, corresponding to a_T for the flow regime in Appendix A, intersects curves 1 and 2 at respective temperatures of 115.9ºC (as can also be seen from Figure 1 above) and 158.5ºC.

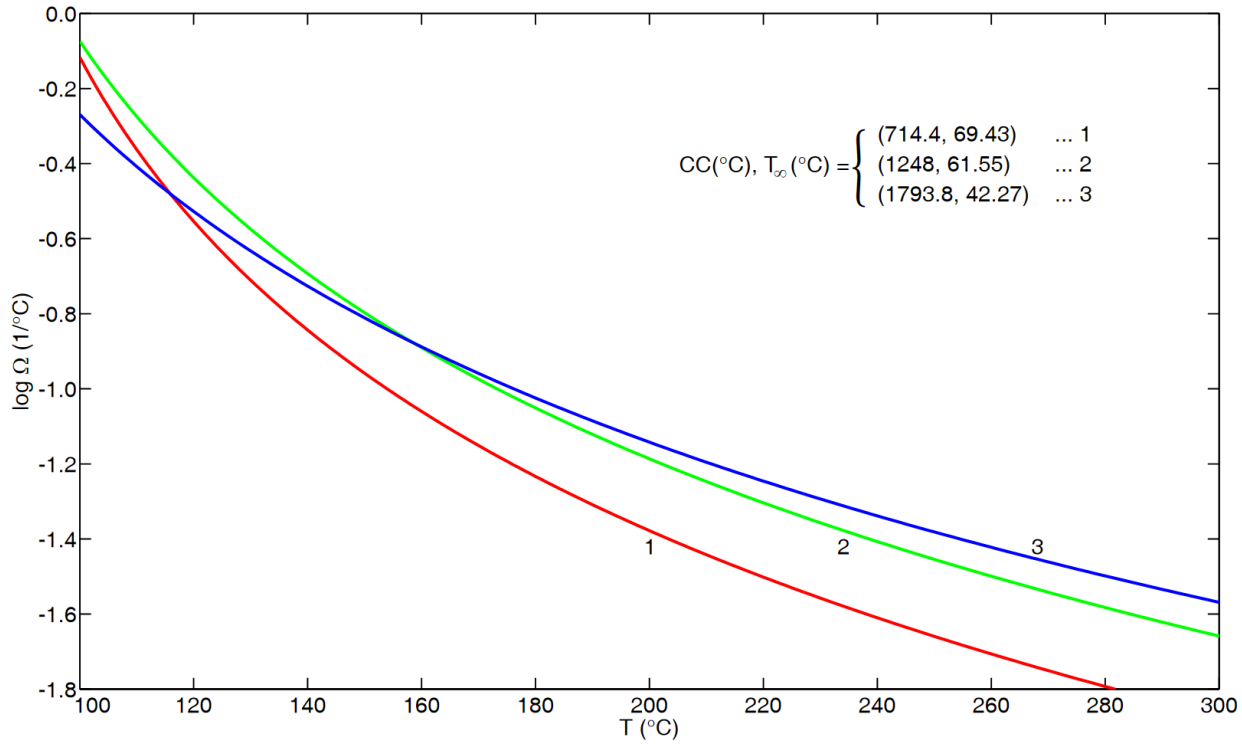

Figure C. Results for Ω versus T based upon three VFTH fits, namely Eqn. (B.2) from Appendix B ("Glass-Rubber Transition"): curve 1 ; (12) from He, et al. [5]: curve 2 ; Eqn. (A.2) from Appendix A ("Flow Regime"): curve 3.

Making use of the three curves in Figure C, one might address some related results in the literature. For example, Figure 3 of He, et al. [5] seems to convincingly indicate that the segmental-correlation time and the viscosity have the same temperature dependence. In particular, the most extensive viscosity results in their Figure 3 is for the "PS-2" polymer, in terms of eight (solid square) data points which range between 1000/T ≅ 2.046/ºK at left and 2.493/ºK at right. Adjusting these points by ΔT_g (= 373ºK − 331ºK = 42ºK, according to their Figure 9 and Table 1) to account for a small M_w of 2310, we are then dealing (in terms of ºC) with respective temperatures of about 257ºC and 170ºC, respectively. Based on Eqns. (A.1) and (A.2) of Appendix A above, it follows that curve 3 in Figure C corresponds to

$$\frac{a_{170°C}}{a_{257°C}} = 2.960 \times 10^2 \qquad (C.1)$$

whereas, from Eqn. (12), curve 2 in Figure C corresponds to

$$\frac{\tau_{seg,c\,(170°C)}}{\tau_{seg,c\,(257°C)}} = 1.678 \times 10^2. \quad (C.2)$$

In particular,

$$2.960 \times 10^2 / 1.678 \times 10^2 = 1.764 = 10^{0.246}. \quad (C.3)$$

 doi:10.20944/preprints202407.0223.v1

That is, according to the tight correlation for the viscosity of PS given by Eqns. (A.1 and A.2) above, the result in (C.3) indicates that the total variation of a_T between the left-most and right-most solid squares in Figure 3 of He, et al. [5] exceeds that of $\tau_{seg,c}(T)$, as given in (12) above, by a factor of 1.764. On a logarithmic basis, as in their Figure 3, this becomes a difference of 0.246 decade. {Note: if a_T in Eqns. (A.1) and (A.2) is replaced by Eqns. (A.1) and (A.3), namely the fit obtained by McKenna et al. [30], the difference becomes 0.263 decade.} Accordingly, such results call into question the correlation for the viscosity and $\tau_{seg,c}$ of polymer d_8PS-2 shown in Figure 3 of [5].

Another concern relates to the relative behavior of the creep compliance and viscosity at higher temperatures. In this regard, one might refer to the work of Ngai [29,32], namely pp. 117/118 from [32] and pp. 262/263 from [29]. In both cases, Ngai first states that, above ≈ 407ºK (134ºC), the (recoverable) creep compliance and viscosity have the same a_T. However, Ngai then qualifies this by indicating that extrapolating creep-compliance data to higher temperatures indicates a weaker temperature dependence than for the viscosity. Unlike in [32], Ngai's corresponding plot in [29], namely Figure 101 (left panel, for PS), explicitly includes a curve for the (recoverable) creep compliance which decays more slowly than that for the viscosity. In turn, this is in agreement with the present results, as shown in Figure C, where curve 1 (corresponding to recoverable-creep compliance) lies below curve 3 (viscous flow) at higher temperatures, namely, above 115.9ºC. Since Ω characterizes the temperature sensitivity, the lower value for curve 1 indicates a slower decay with increasing temperature.

Appendix D: Calculating Ω(1/ºC) at Moderate M_w

Based upon Eqns. (3) {with "τ_{eq}" replaced by "τ_α"} and (13), it follows that

$$\Omega = \ln 10 \times \frac{m}{T_g(^\circ K)} \quad \text{(D.1)}$$

where Ω(1/ºK) or, equivalently, Ω(1/ºC). Hence, based on the values for m (fragility index) presented by Hintermeyer, et al. [23] in their Figures 5(c), 6(c) and 7(c) for PDMS, PS and PB, respectively, with corresponding values for T_g(ºK) from their Tables 1, 2 and 3, resulting values are presented in Tables D-1, D-2 and D-3 below for Ω(1/ºC) as a function of M_w.

Table D-1. Ω(1/ºC) results for PDMS, based on Eqn. (D.1) and Table 1 & Figure 5(c) of Hintermeyer, et al. [23].

M_w	T_g(ºK)	m	Ω(1/ºC)
311	126.3	107.1	1.95
311	126.3	116.1	2.12
860	133.6	100.9	1.74
1600	138.2	108.0	1.80
1600	138.2	110.0	1.83
2490	139.9	110.0	1.81
3510	141.5	111.0	1.81
4560	142.4	111.4	1.80
5940	143.0	113.2	1.82
11.0K	144.0	115.1	1.84
21.6K	144.2	113.6	1.81
41.4K	144.5	114.1	1.82
128K	144.4	116.1	1.85
232K	144.6	115.0	1.83

 doi:10.20944/preprints202407.0223.v1

Table D-2. Ω(1/ºC) results for PS based upon Eqn. (D.1) and Table 2 & Figure 6(c) of Hintermeyer, et al. [23].

M_w	T_g(ºK)	m	Ω(1/ºC)
106	114.7	81.6	1.64
162	138.9	76.8	1.27
370	231.9	78.0	0.77
690	261.4	72.1	0.64
1350	314.2	97.0	0.71
3250	347.0	107.5	0.71
8900	356.9	105.4	0.68
19.1K	367.9	116.2	0.73
33.5K	369.0	119.6	0.75
96.0K	372.6	120.9	0.75
243K	373.3	122.6	0.76
546K	372.0	122.0	0.76

Table D-3. Ω(1/ºC) results for PB based upon Eqn. (D.1) and Table 3 & Figure 7(c) of Hintermeyer, et al. [23].

M_w	T_g(ºK)	m	Ω(1/ºC)
355	140.9	70.0	1.14
466	161.2	71.1	1.02
575	162.1	73.0	1.04
777	165.3	78.0	1.09
1450	170.7	81.1	1.09
2020	173.6	83.0	1.10
2760	174.5	88.0	1.16
4600	174.0	90.9	1.20
19.9K	175.3	90.0	1.18
35.3K	174.5	90.9	1.20
87.0K	174.4	90.5	1.19

References

1. Hieber, C.A. Modelling the Density Relaxation of Polystyrene. *Rheol Acta* **2022**, *61*, 523-538**.**
2. O'Connell, P.A.; McKenna, G.B. Arrhenius-type Temperature Dependence of the Segmental Relaxation Below Tg. *J. Chem Phys* **1999**, *110(22)* 11054-11060**.**
3. Zhao, J.; McKenna, G.E. Temperature Divergence of the Dynamics of a Poly (vinyl acetate) Glass: Dielectric vs. Mechanical Behaviors. *J. Chem Phys* **2012**, *136*, 154901.
4. Roland, C.M.; Casalini, R. Temperature Dependence of Local Segmental Motion in Polystyrene and its Variation with Molecular Weight. *J. Chem Phys* **2003**, *119*(*3*), 1838-1842**.**
5. He, Y.; Lutz, T.R.; Ediger, M.D.; Ayyagari, C.; Bedrov, D.; Smith, G.D. NMR Experiments and Molecular Simulations of the Segmental Dynamics of Polystyrene. *Macromolecules* **2004**, *37(13)*, 5032-5039.
6. Vogel, H. Das Temperatur-Abhangigklitsgersetz der Viskosität von Flüssigkeiten. *Phys Z* **1921**, *22*, 645-646**.**
7. Fulcher, G.S. Analysis of Recent Measurements of the Viscosity of Glasses. *J Am Ceram Soc* **1925**, *8(6)*, 339-355**.**
8. Tammann, G.; Hesse, W. Die Abhängegkeit der Viskosität von der Temperatur bei Unterkühlten Flüssigkeiten. *Z Anorg Allg Chem* **1926**, *156*, 245-257**.**

9. Plazek, D.J. Temperature Dependence of the Viscoelastic Behavior of Polystyrene. *J. Phys Chem* **1965**, *69(10)*, 3480-3487.
10. Zosel, J. Der Einfluss von Molekulargewicht und Molekulargewichtsverteilung auf die Viskoelastischen Eigenschaften von Polystyrolschmelzen. *Rheol Acta* **1971**, *10(2)*, 215-224.
11. Marin, G.; Graessley, W. Viscoelastic Properties of High Molecular Weight Polymers in the Molten State; 1: Study of Narrow Molecular Weight Distribution Samples. *Rheol Acta* **1977**, *16(5)*, 527-533.
12. Schausberger, A.; Schindlauer, G.; Janeschitz-Kriegl, H. Linear Elastico-Viscous Properties of Molten Standard Polystyrenes; I: Presentation of Complex Moduli; Role of Short Range Structural Parameters. *Rheol Acta* **1985**, *24(3)*, 220-227.
13. Lomellini, P. Williams-Landel-Ferry Versus Arrhenius Behavior: Polystyrene Melt Viscoelasticity Revised. *Polymer* **1992**, 33(23), 4983-4989.
14. Aklonis, J.J.; Tobolsky, A.V. Stress Relaxation and Creep Master Curves for Several Monodisperse Polystyrenes. *J. Appl Phys* **1965**, *36(11)*, 3483-3486.
15. Plazek, D.J.; O'Rourke, V.J. Viscoelastic Behavior of Low Molecular Weight Polystyrene. *J. Polym Sci, part A2*, **1971**, *9(2)*, 209-243.
16. Plazek, D.J.; Agarwal, P. Comparison of Similar Narrow Molecular Weight Polystyrenes. *J. Appl Polym Sci* **1978**, *22(8)*, 2127-2135.
17. Schwarzl, F.R.; Zahradnik, F. The Time Temperature Position of the Glass-Rubber Transition of Amorphous Polymers and the Free Volume. *Rheol Acta* **1980**, *19(2)*, 137-152.
18. Link, G.; Schwarzl, F.R. Shear Creep and Recovery of a Technical Polystyrene. *Rheol Acta* **1987**, *26(4)*, 375-384.
19. Angell, C.A. Relaxation in Liquids, Polymers and Plastic Crystals – Strong/Fragile Patterns and Problems. *J. Non-Cryst Solids* **1991**, *131-133*, 13-31.
20. Lindsey, C.P.; Patterson, G.D.; Stevens, J. Photon Correlation Spectroscopy of Polystyrene Near the Glass-Rubber Relaxation. *J. Polym Sci (Polym Phys Ed)* **1979**, *17(9)*, 1547-1555.
21. Lee, H.; Jamieson, A.M.; Simha, R. Photon Correlation Spectroscopy of Polystyrene in the Glass Transition Region. Macromolecules **1979**, *12(2)*, 329-332.
22. Pschorn, U.; Rössler, E.; Sillescu, H.; Kaufmann, S.; Schaefer, D.; Spiese, H.W. Local and Cooperative Motions at the Glass Transition of Polystyrene: Information from One- and Two-Dimensional NMR as Compared with Other Techniques. *Macromolecules* **1991**, *24(2)*, 398-402.
23. Hintermeyer, J.; Herrmann, A.; Kahlau, R.; Goiceanu, C.; Rössler, E.A. Molecular Weight Dependence of Glassy Dynamics in Linear Polymers Revisited. *Macromolecules* **2008**, *41(23)*, 9335-9344.
24. Patterson, G.D.; Carroll, P.J.; Stevens, J.R. Photon Correlation Spectroscopy of Polystyrene as a Function of Temperature and Pressure. *J. Polym Sci (Phys)* **1983**, *21(4)*, 605-611.
25. Boyd, R.H.; Smith, G.D. *Polymer Dynamics and Relaxation*. Cambridge University Press: New York, NY, USA **2007.**
26. Ferry, J.D. *Viscoelastic Properties of Polymers* (3rd Ed). Wiley: New York, NY, USA **1980.**
27. Williams, M.L.; Landel, R.F.; Ferry, J.D. The Temperature Dependence of Relaxation Mechanisms in Amorphous Polymers and Other Glass-Forming Liquids. *J. Am Chem Soc* **1955**, *77*, 3701-3707.
28. Ngai, K.L. *Relaxation and Diffusion in Complex Systems*, Springer, New York, NY, USA, **2011.**
29. Nelder, J.A.; Mead, R. A Simplex Method for Function Minimization. *Comput J* **1965**, *7(4)*, 308-313.
30. McKenna, G.B.; Hadziioannou, G.; Lutz, P.; Hild, G.; Strazielle, C.; Straupe, C.; Rempp, P.; Kovacs, A.J. Dilute Solution Characterization of Cyclic Polystyrene Molecules and Their Zero-Shear Viscosity in the Melt. *Macromolecules* **1987**, *20(3)*, 498-512.
31. Ngai, K.L. In *Physical Properties of Polymers*, 3rd ed.; Mark, J., Ngai, K., Graessley, W., Mandelkern, L., Samulski, E., Koenig, J., Wignall, G., Eds.; Cambridge University Press: Cambridge, UK, **2004**, 72-152.